

Control of Vibrations in a Micromechanical Gyroscope Using Inertia Properties of Standing Elastic Waves

N. Ovchinnikova, A. Panferov, V. Ponomarev, L. Severov

*Department of Aerospace Instruments of orientation, navigation and stabilization
Saint-Petersburg University of Aerospace Instruments, Saint-Petersburg, RUSSIA
e-mail: panferov@aanet.ru*

Abstract: The characteristics of the dynamics and control of oscillations in a micromechanical ring resonator gyro that uses inertia properties of elastic waves are considered. A functional diagram of the gyroscope with a ring resonator is presented. Further, the scheme has a loop oscillation excitation and a measurement channel. This model is studied under the excitation of the resonator, which automatically provides maximum vibration amplitude with minimum control. It is shown that the using the schemes of stabilization of of the excited amplitude or normalisation secondary oscillations significantly reduces the non-linear characteristics of the transformation. To achieve the desired dynamic characteristics of the gyroscope, it is proposed to use feedback in the measuring channel by the velocity of radial displacement of the ring resonator in the output zone. The technique allows the calculation of the envelope of the fundamental mode oscillation from appropriate differential equations. That is a convenient tool for a comparative investigation of the gyro's characteristics while studying the direct measurement type and the compensation type.

Keywords: MEMS, micromechanical gyroscope, elastic wave resonator, basic theory, direct conversion mode, compensation of the Coriolis forces

1. INTRODUCTION¹

Most of currently used micromechanical angular velocity sensors are constructed according to the scheme of vibratory gyroscope (Ayazi F., Najafi K. 2000), (Zarabadi S. A 1999), (Hopkin I. 1997). A construction, in which the inertia properties of the ring resonator excited into standing waves is exploited, has received relatively much less attention.. At present, the company Silicon Sensing (UK) specialize in the production of such gyroscopes (MMG R- type). Developers find that R-type gyroscopes have the best characteristics of noise and vibration resistance in class devices. Gyroscopes work like angular velocity sensors when excitation resonator is positional. It means that the profile of the radial forces is rigidly attached to the case and corresponds to the basic oscillation elliptical shape see, for example, (Zhuravlev V.F., Klimov D.M. 1985), (Matveev V.L. 1998), (Lunin B.S. 2005), (Mercuriev I.V. 2009). There are two types of oscillations (primary and secondary) for different micromechanical vibratory gyroscope designs. Primary oscillations generated by the excitation system, and the secondary ones appear because of the Coriolis force during rotation of the base. The frequency difference between the primary and secondary oscillations is a parameter that significantly affects the main metrological characteristics of the device. Therefore, it is necessary to take special measures to stabilise the frequency difference, or combine them. In wave gyroscopes no such problem is encountered, since the

primary and the secondary oscillations have the same frequency. These are benefits of the standing wave gyroscope concept over of the vibrating gyroscopes. On other hand, the dynamics of bending oscillations for ring resonator are described by the non-homogeneous partial differential equations. In this case, the heterogeneity of equations is determined by a continuous action of the excitation oscillations and other control forces (if the device is in the compensation mode). The peculiarity of the wave gyroscopes is that the angular velocity to be measured enters into the wave equation in the form of changing coefficients. General solution of this equation does not exist. To evaluate the dynamic characteristics of wave gyroscopes, the most convenient forms of approximate solutions of the wave equations are to study the dynamics of the main modes of oscillations and to get the original model for the formation reading the values systems and control fluctuations. The present article addresses the key issues of the wave theory of micromechanical gyroscopes with a ring resonator and explores ways to achieve the required metrological characteristics of the devices in the direct measurement and compensation type, the source of measurement errors for such gyros.

2. FUNCTIONAL SCHEME OF THE ANGULAR VELOCITY SENSOR

The generalized block scheme of a micromechanical sensor of angular velocity, which as a sensing element used in the form of a ring resonator, is shown on Fig 1. The resonator is circumferentially surrounded by eight electrodes as numbered in the figure. The electrodes 1 and 5 form a capacitive sensor of radial displacement of the ring in a zone of primary

¹ This study was supported by Russian Foundation for BasicResearch, project 13-08-01016

oscillations, and with the electrodes 3 and 7 are electrically forces ensuring the generation of the primary oscillations. Similarly, the electrodes 2 and 6, as well as electrodes 4 and 8 form a system used for measuring and controlling the secondary oscillations.

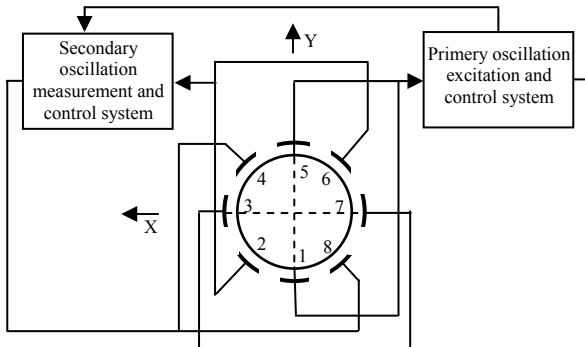


Fig.1 Functional scheme of the angular velocity sensor

The circuitry of the excitation system and control primary oscillations and the measurement system and control of secondary oscillations depends on the choice of the primary ways of exciting variations and ways to generate output signals of the device. This may be implemented as a direct conversion mode thus compensating the measurement mode.

The physical basis of the occurrence of secondary oscillations are described in the literature (Panferov A.I., Ponomarev V.K., 2011).

3. THE DYNAMIC EQUATIONS OF THE RING RESONATOR

In the linear theory of elasticity the dynamics of the ring resonator is described the following partial differential equation (Zhuravlev V.F. Klimov D.M. 1985), (Severov L.A. 1996) which is second order in time and fourth order in the variable φ .

$$\ddot{w}^{II} - \dot{w} + 4\Omega\dot{w}^I + 2\dot{\Omega}w^I + \xi_1(\dot{w}^{VI} + 2\dot{w}^{IV} + \dot{w}^{II}) + \chi^2(w^{VI} + 2w^{IV} + w^{II}) = f(t, \varphi) = p_B(t, \varphi) + p_K(t, \varphi), \quad (1)$$

where w is the radial displacements of points on resonator center line; $\dot{w} = \frac{dw}{dt}$; $w^I = \frac{\partial w}{\partial \varphi}$; Ω - sensed angular

velocity; p_B and p_K - reduced forces of the excitation and controlled factors.

Structural parameters being part of equation (1) determining elastic and damping forces at ring rectangular cross-section are found under the formulas:

$$\chi^2 = \frac{Eh^2}{12\rho R^4}, \quad \xi_1 = \frac{\xi h^2}{12\rho R^4}, \quad (2)$$

where E , ρ are the elasticity modulus and the ring material density, R and h are the center line radius and the thickness of ring, ξ is the coefficient of viscous damping forces.

The general solution of equation (1) is represented by an infinite series of harmonics (vibration modes), each of which retains the properties of inertia in space. The greatest weight

in the radial displacement of the points of the ring makes a second mode of oscillation. To obtain the equation for the second (main) modes of oscillation, Bubnov-Galerkin solution will be sought in the following form

$$w(t, \varphi) = C(t)\cos 2\varphi + S(t)\sin 2\varphi. \quad (3)$$

and reduced external forces are expanded in a similar form but with two new time-varying coefficients:

$$f(t, \varphi) = f_1(t)\cos 2\varphi + f_2(t)\sin 2\varphi. \quad (4)$$

After evaluating the partial derivatives of equation (3) and substituting them into equation (1) with regard to the expression (4) while noting that $\Omega = \text{Const}$, we have:

$$5\ddot{C}(t)\cos 2\varphi + 5\ddot{S}(t)\sin 2\varphi + 8\Omega\dot{C}\sin 2\varphi - 8\Omega\dot{S}\cos 2\varphi + 36\chi^2 C(t)\cos 2\varphi + 36\chi^2 S(t)\sin 2\varphi = -f_1 \cos 2\varphi - f_2 \sin 2\varphi.$$

Separating oscillations two modes of oscillations corresponding to the sines and the cosines respectively, we obtain the following set of two coupled ordinary differential equation in the time variable and note that the spatial variable has been eliminated from the dynamics because of the application of the Bubnov-Galerkin approach

$$\begin{aligned} \ddot{C}(t) - \frac{8}{5}\Omega\dot{S}(t) + \frac{36}{5}\xi_1\dot{C}(t) + \frac{36}{5}\chi^2 C(t) &= -0.2f_1; \\ \ddot{S}(t) + \frac{8}{5}\Omega\dot{C}(t) + \frac{36}{5}\xi_1\dot{S}(t) + \frac{36}{5}\chi^2 S(t) &= -0.2f_2. \end{aligned} \quad (5)$$

The first equation describes oscillations relative axes OX and OY, the second one - relative the axes rotated by an angle of 45°. The first of these axes are the excitation axes of the primary oscillations, while the latter are measuring axes (axes of the secondary oscillations).

In the absence of angular velocity term equation (5) can be integrated independently as the two equations decouple - thus illustrating the gyroscopic coupling between the two motions which arise from Coriolis effects.

Equation (5) can be written in a standard form:

$$\ddot{C}(t) - 1.6\Omega\dot{S}(t) + 2\zeta\nu\dot{C}(t) + \nu^2 C(t) = -0.2f_1; \quad (6)$$

$$\ddot{S}(t) + 1.6\Omega\dot{C}(t) + 2\zeta\nu\dot{S}(t) + \nu^2 S(t) = -0.2f_2, \quad (7)$$

where $\nu = \frac{6}{\sqrt{5}}\chi$ - own frequency of the second oscillation mode;

$$\zeta = 0.6\sqrt{5} \frac{\xi_1}{\chi} - \text{rate of oscillation.}$$

Equations (6) and (7) describe vibrations of the resonator and can be treated as the mathematical model for the analysis and design of a micromechanical gyroscope as a single electromechanical system.

Gyroscopes with a ring resonator, as well as other micro-mechanical gyroscopes, are modulation type devices. The information parameter is the amplitude (envelope) of the oscillations. To obtain the equations describing the dynamics of envelope, the forced oscillation being at the excitation frequency in the steady state and the own frequency of the

resonator, the general solution of equation (1) will be sought in the form:

$$W(t, \varphi) = [a(t)\cos 2\varphi + b(t)\sin 2\varphi]\cos vt + [m(t)\cos 2\varphi + n(t)\sin 2\varphi]\sin vt. \quad (8)$$

Electrostatic excitation forces and control of oscillations can be expressed in the following form

$$p_B(t, \varphi) = q_B^H(t, \varphi) = f_0 \cos vt \cos 2\varphi, \quad (9)$$

$$p_K(t, \varphi) = q_K^H(t, \varphi) = f_K \cos vt \sin 2\varphi.$$

Substituting (8) and (9) into equation (1) and dividing the oscillation modes, the system of equations are obtained as a set of four second order coupled ordinary differential equations with constant coefficients ($\Omega = const$):

$$\ddot{a} = \left(v^2 - \frac{36}{5}\chi^2\right)a - 7.2\xi_1\dot{a} + 1.6\Omega\dot{b} - 7.2\xi_1vm - 2v\dot{m} + 1.6\Omega vn + 0.2f_0; \quad (10)$$

$$\ddot{b} = -1.6\Omega\dot{a} + \left(v^2 - \frac{36}{5}\chi^2\right)b - 7.2\xi_1\dot{b} - 1.6\Omega vm - 7.2\xi_1vn - 2v\dot{n} - 0.2f_K;$$

$$\ddot{m} = 7.2\xi_1va + 2v\dot{a} - 1.6\Omega vb + \left(v^2 - \frac{36}{5}\chi^2\right)m - 7.2\xi_1m + 1.6\Omega n;$$

$$\ddot{n} = 1.6\Omega va + 7.2\xi_1vb + 2v\dot{b} - 1.6\Omega\dot{m} + \left(v^2 - \frac{36}{5}\chi^2\right)n - 7.2\xi_1\dot{n}.$$

In the steady state, and in the absence of control forces, the oscillation will be:

$$\begin{aligned} (5v^2 - 36\chi^2)a - 36\xi_1vm + 8\Omega vn &= f_0; \\ (5v^2 - 36\chi^2)b - 8\Omega vm - 36\xi_1vn &= 0; \\ 36\xi_1va - 8\Omega vb + (5v^2 - 36\chi^2)m &= 0; \\ 8\Omega va + 36\xi_1vb + (5v^2 - 36\chi^2)n &= 0. \end{aligned} \quad (11)$$

If consider that $5v^2 - 36\chi^2 = 0$ will have: $a = b = 0$,

$$m = \frac{f_0 36\xi_1}{v[(36\xi_1)^2 + (8\Omega)^2]}; \quad (12)$$

$$n = \frac{f_0 8\Omega}{v[(36\xi_1)^2 + (8\Omega)^2]}. \quad (13)$$

Parameters m and n are the amplitudes of the resonator in the excitation and measurement modes.

The dependences obtained above show that the angular velocity amplitudes of the base causes the resonator in the measuring zone, and in the zone of excitation. Moreover the non-linear nature of these relationships are apparent.

4. THE EXCITATION OF THE RESONATOR'S OSCILLATIONS

The wave resonator oscillation is excited by the application of a periodic force from the force sensors located in the excitation zone. The amplitude of the excited oscillations will be maximised if the frequency of the periodic excitation force coincides with the natural frequency of the mechanical resonance. There are two possible ways to provide excitation

to achieve resonance in micromechanical vibratory gyroscopes:

- excitation of oscillations in self-maintained mode;
- excitation with master or reference generator whose frequency is automatically tuned to mechanical resonance frequency.

The second approach, for instance, is implemented in Silicon Sensing (Ayazi F., Najafi K. 2000).

To implement the first method, a technically simple way of positive feedback by sign of resonator element motion speed in the area of excitation electrodes location is ensured. Additional energy added by this way should prevail over that of dissipative forces resulting in oscillations development. Amplitude of steady oscillations is restricted by maximum exciting force. The maximum use of output performance of force sensors will be achieved by this way, in which the force sensor works in a relay mode (Severov L.A., Ponomarev V.K. 2011). A functional scheme of self-oscillating field system that implements the method of formation of the excitation pulses is shown in Figure 2.

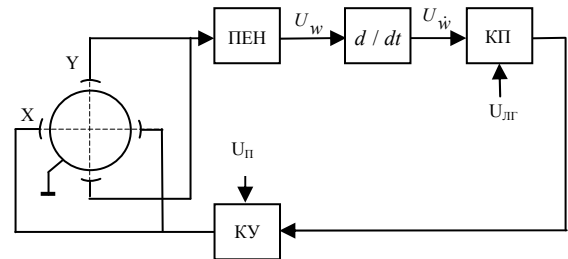


Fig.2 Functional scheme of the resonator excitation self-oscillator system

In Fig. 2, two gyroscope electrodes located at axis y and connected in parallel are used for the measurement of resonator displacement, and two electrodes at the x -axis – as a force sensor.

In the autogenerating exciting force (as mentioned) is formed under the law

$$f_1(t) = f_0 \text{sign} \dot{C}(t). \quad (14)$$

Thus, the model of resonator in self-maintained mode is described by the following equations:

$$\ddot{C}(t) - 1.6\Omega\dot{S}(t) + 2\zeta v\dot{C}(t) + v^2 C(t) = -0.2f_0 \text{sign} \dot{C}(t);$$

$$\ddot{S}(t) + 1.6\Omega C(t) + 2\zeta v S(t) + v^2 S(t) = 0,$$

where f_0 - the maximum value of the specific force excitation electrodes.

When $\Omega = 0$, the excitation process describes only the first equation of system (15). For a first approximation of its solutions, keeping in mind the physical picture of the circuit, we assume that the sensor applies a force to the resonator harmonic effects with a frequency equal to the natural frequency of the resonator [Hopkin I. (1997)]. Then the above equation becomes:

$$\ddot{C}(t) + 2\zeta v\dot{C}(t) + v^2 C(t) = -0.2f_0 \sin vt. \quad (16)$$

Given the smallness of the parameter ζ , the solution of equation (16) can be found in the form:

$$C(t) = \frac{0.1f_0}{2\zeta v^2} (e^{-a} - 1) \cos vt,$$

where $a = v\zeta = 3.6\xi_1$.

The amplitude of the steady-state oscillation is equal to

$$A_c = \frac{0.1f_0}{2\zeta v^2}.$$

The same result can be obtained in case of equation (10) for the envelope of the resonator. In this case, the reduced excitation force should be written as

$$f_0 = f_0 \text{sign}(\dot{a} + v m).$$

Since the implementation of the autogenerating way to excite oscillations disturbing force is not harmonic signal, and a binary sequence, the result should be corrected by adjusting the shape of the excitation signal.

Thus
$$A_c = \frac{0.1 \cdot K_d}{\zeta v^2},$$

where
$$K_d = \sqrt{\frac{\pi}{2}} \approx 1.25.$$

The temporal response showing the build-up of the amplitude within an envelope, of the physical resonator whose dynamics are described by equations (16), is presented in Figure 3. Figure 4 shows changes in the amplitude of oscillations, resulting from the numerical solutions of equations (10) for the envelope fluctuations. Both graphs correspond to the case of an unmoving base ($\Omega = 0$).

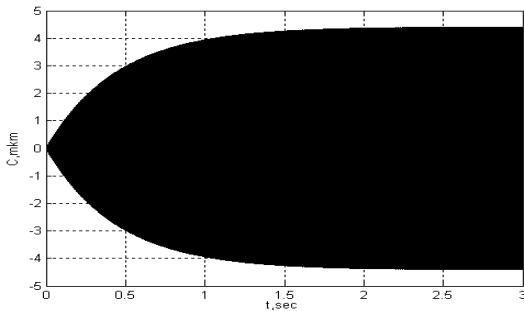


Fig.3 The temporal development of oscillations of the resonator in the absence of base rotation

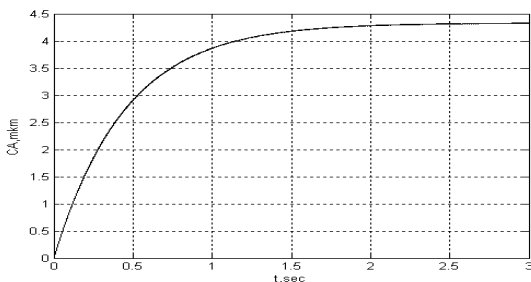


Fig.4 Change of amplitude of oscillations in the absence of rotation of the base

If base is rotating ($\Omega \neq 0$), the oscillation amplitude of the resonator are given by equation (12). A comparison of the envelope as numerically calculated from the direct numerical integration with those obtained analytically for the envelope can be made from Fig.5 and Fig.6. respectively.

The results of studies suggest that besides the dependence of the amplitude of the excited oscillations and the angular velocity of the base the time to build up the oscillations is large enough which affects the time the device operational readiness.

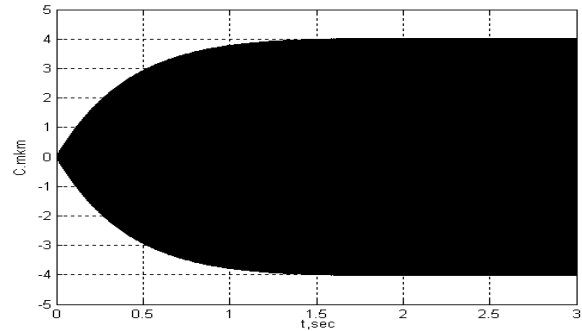


Fig.5 The development of oscillations in the presence of the rotation of the base

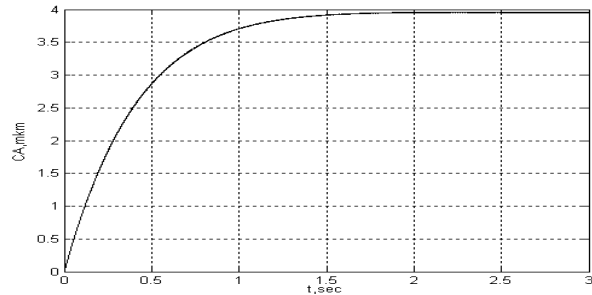


Fig.6 The change in the amplitude of oscillations in the presence of rotation base

5. FORMATION OF THE MEASUREMENT CHANNEL TO THE ANGULAR VELOCITY SENSOR DIRECTLY MEASURING

As MEMS vibratory gyroscopes produce a velocity signal as a response to the rotation of the base, synchronous detection with a reference oscillatory signal generated in the excitation circuit is necessary. However, a significant non-linearity in the characteristics of transformation must be considered. This is given by a formulaic relationship (13).

Using (12) and (13) we obtain

$$n = m \frac{8}{36\xi_1} \Omega.$$

Thus, when no rotational angular velocity of the base oscillation is present, the amplitude of the resonator in the excitation zone is maintained constant and is equal to the nominal value; the amplitude of vibrations in the measurement zone is related to the linear dependence of the measured quantity

$$n = m_0 \frac{8}{36\xi_1} \Omega = k_n \Omega,$$

where k_n - conversion factor of the resonator.

If there is power, the margin of force gage of the excitation system amplitude stabilization may sufficiently reduce the impact on the metrological parameters of the device measuring excitation factors.

One may realize the stabilization of resonator oscillations through a change of feed voltage of the key magnifier, which principally is shown in Fig.2.

Controller of the amplitude stabilization system can be constructed, for example, according to the scheme in which an amplitude detector, a low pass filter correction circuit and a buffer amplifier [Severov L.A., Ponomarev V.K., and Other, (2011c)] is used.

Following amplitude stabilization, accumulator register stabilization of the error signal is established. Through correction contour CC and buffer amplifier BA, at input of which current stabilization voltage is formed, signal enters the control input of voltage stabilizer VS of key magnifier of excitation system. Selection of the structure of correction contour provides the required static and dynamic characteristics of the system [Severov L.A., Ponomarev V.K. (2011)].

As an illustration, in Fig. 7 shows the transitive processes in the contour of autoexcitation during actuation of contour of amplitude stabilization. Fig. 7a shows the pattern of development of physical oscillations and Fig. 7b – identified by amplitude detector and phase-sensitive rectifier enveloping curve (amplitude) of oscillations.

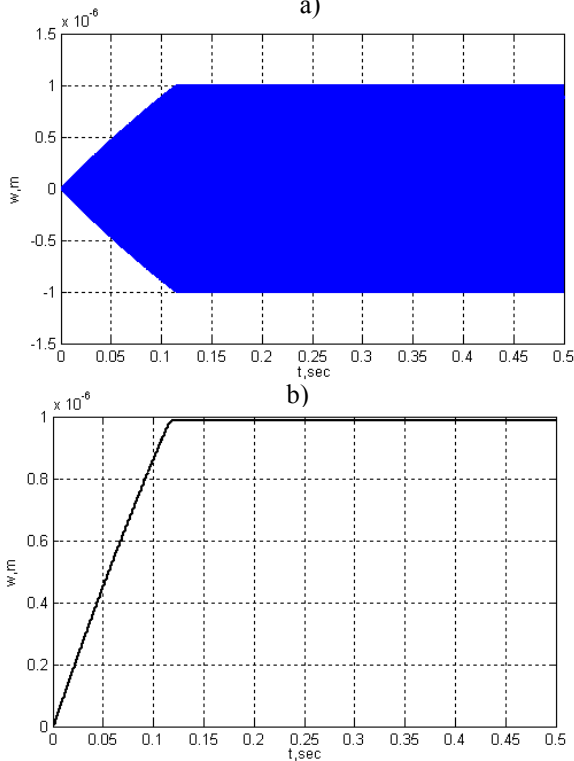


Fig. 7 Transitive processes in the contour of autoexcitation during actuation of contour of amplitude stabilization

As can be seen, the time of operational readiness of the device significantly decreases. Additional investigations have shown that there is substantial smoothing of gyroscope calibration.

The linear conversion characteristic can be obtained via normalization operations by selecting the amplitude to the measuring axis vibration amplitude along the axis of the excitation

$$n = \frac{n}{m} = \frac{8}{36\xi_1} \Omega = k_{n1} \Omega. \quad (17)$$

If the device is implemented stabilization mode excitation amplitude oscillations, the dynamic characteristics of the measuring channel will be described by the equation

$$\ddot{S}(t) + 2\zeta v \dot{S}(t) + v^2 S(t) = 1.6 A_c v \Omega(t) \sin vt. \quad (18)$$

The solution of this equation in the quasi-constant function $\Omega(t) = \Omega_0 = \text{const}$ will be

$$S(t) = \frac{0.8 A_c}{\zeta v} (e^{-at} - 1) \Omega_0 \cos vt. \quad (19)$$

As can be seen, the envelope of fluctuations varies exponentially, which makes it possible to describe the dynamics of an aperiodic transfer function.

$$W_{As}^\Omega(p) = \frac{k_n}{(T_m p + 1)}, \quad (20)$$

where $k_n = \frac{0.8 A_c}{\zeta v}$, and $T_m = \frac{1}{a}$.

The transfer function (20) and the corresponding frequency response will determine the dynamic characteristics of the angular velocity sensor for a direct measurement in the frequency band of measurement.

In an embodiment of the device, the normalization of the output dynamic characteristics can be established only in the model experiment, because the procedure of normalization is a nonlinear operation. Thus, the dynamic characteristics of the gyro will depend on the magnitude of the measured angular velocity. To the greatest extent, it is shown in the measurement of large angular velocities (Fig. 8)

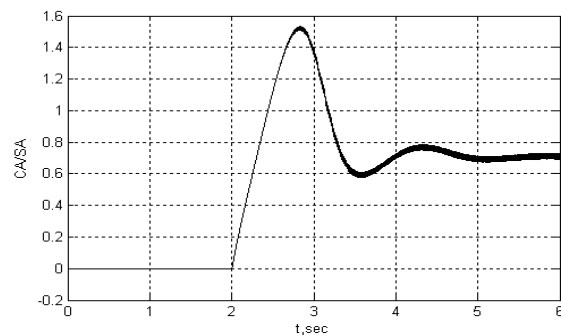


Fig. 8 Dynamics of the output signal in the measurement of large angular velocity

6. COMPENSATION MEASUREMENT MODE

The main objective of compensating mode measurement is to provide dynamic performance requirements on the device and, in particular, the requirements for the working frequency band. This can be obtained by using feedback by velocity of ring elements movement in output zone.

While maintaining the amplitude of the oscillation perturbed by constant dynamic measurement channel, taking into account the forces that compensate for the Coriolis force, the dynamical equation for oscillations relative the axes rotated by an angle of 45° to axes OX and OY is given by

$$\ddot{S}(t) + 2\zeta v \dot{S}(t) + v^2 S(t) = 1.6 A_c v \Omega_0 \sin vt - 0.2 f_{2_0} k_{oc} \dot{S}(t). \quad (21)$$

where f_{2_0} - energy parameter of the force sensor; k_{oc} - transfer coefficient of compensation loop.

The solution of the equation (21) can be expressed as

$$S(t) = \frac{0.8 A_c}{\zeta_1 v} \left(e^{-\zeta_1 vt} - 1 \right) \Omega_0 \cos vt,$$

where $\zeta_1 = \zeta + \frac{0.2 f_{2_0} k_{oc}}{2v}$.

The solution shows that time constant of transition is increasing when k_{oc} decreases. That is why the working band frequencies of the device is widening. Using these relationships and making the requirements for the working frequency band, the necessary coefficient of the feedback compensation loop of the Coriolis forces can be found.

CONCLUSIONS

The investigation described in this paper shows that the angular velocity sensor with ring resonator and positional excitation without the system for oscillations control possesses unsatisfactory technical characteristics of linear transformation, working frequency band, time of readiness. These characteristics can be improved when compensating measurement mode is employed. It has been shown that another efficient means of improvement of transformation linearity and shortening of readiness time is an arrangement of stabilization contour of resonator oscillations amplitude in the excitation zone. Here, the task of the oscillations control contour in the data recording zone (compensation contour) is provision of required working band of sensor frequencies.

Ayazi F., Najafi K. (2000) High Aspect-ratio Dry-Release Poly-Silicon MEMS Technology For Inertial-Grade Microgyroscopes *Position Location and Navigation Symposium*, San Diego, California. p. 304-308.

Zarabadi S. A (1999) Resonating Comb/Ring Angular Rate Sensor, Delphi Delco Electronics Systems, Sensors and Actuators. (SP-1443).

Hopkin I. (1997) Performance and Design of Silicon Micromachined Gyro. // *Symposium Gyro Technology*, Germany. 1997. P. 1.0-1.10.

Fell C.P., Hopkin I., Townsend K., Sturland I. (1999) A Second Generation Silicon Ring Gyroscope // *Symposium Gyro Technology*, Germany.

Zhuravlev V.F. Klimov D.M. (1985) Wave solid-state gyroscope of M: Science. 126 p.(in Russian)

Matveev V. L. Lipatnikov V. I. Alekhin A.V. (1998) Design of a wave solid-state gyroscope of M: MGTU. 168 c. (in Russian)

Lunin B. S. (2005) Physical and chemical bases of development of hemispherical resonators of wave solid-state gyroscopes. M: MAI, (in Russian)

Merkuriev I.V. Podalkov V.V. (2009) Dynamics of the micromechanical and wave solid-state gyroscopes. *Physmatlit*, 225 p. (in Russian)

Severov L.A. (1996) Mechanics of gyroscopic systems. M, MAI, 212c. (in Russian)

Severov L.A., Ponomarev V.K., Panferov A.I., Ovchinnikova N.A. (2010) Angular Velocity Sensors Based on Ring Resonator. *Proceedings of 2010 International Symposium on Inertial Technology and Navigation ISITN*. Nanjing, China, October, p. 58-66

Panferov A., Ponomarev V., Nebylov V. (2011) Filtering and parameters estimation in gyros with an elastic suspension. *Proceedings 5-th International Scientific Conference on Physics and control. PhysCon*. <http://lib.physcon.ru/doc?id=a8bd55dbaddb>

Panferov A.I., Ponomarev V.K., Severov L.A. (2011) Angular rate sensors based on the MEMS ring resonators. *Proceedings 5-th International Scientific Conference on Physics and control. PhysCon*., <http://lib.physcon.ru/doc?id=e21f6b87508a>

Panferov A.I., Ponomarev V.K. (2012) Algorithms for Embedded Controllers in Microgyros. *Proceedings of IFAC-EGNCA*. Paper ID 474

Severov L.A., Ponomarev V.K., Panferov A.I., Ovchinnikova N.A. (2011) Configuration and Characteristics of the Angular velocity Sensor Based on the wave Solid-state gyroscope with the Ring Resonator. *17th Saint Petersburg International Conference on Integrated Navigation Systems*. Saint Petersburg. State Research.Center of the Russian Federation Concern Elestopribor, JSC. pp 134-141.